International Journal of Mechanical Engineering and Applications
2014; 2(1): 11-17
Published online January 30, 2014 (http://www.sciencepublishinggroup.com/j/ijmea)
doi: 10.11648/j.ijmea.20140201.13

Relaxation and conduction mechanisms of high T_c lead-free Ba (Zr,Ti)O_3 positive temperature coefficient of resistivity ceramic using impedance spectroscopy

Md. Azizar Rahman[1, *], Abdul Quader[2], A. K. M. Akther Hossain[1]

[1]Department of Physics, Bangladesh University of Engineering and Technology, Dhaka, Bangladesh
[2]Faculty of Engineering & Technology, Eastern University, Dhaka, Bangladesh

Email address:
azizar@phy.buet.ac.bd (M. A. Rahman)

To cite this article:
Md. Azizar Rahman, Abdul Quader, A. K. M. Akther Hossain. Relaxation and Conduction Mechanisms of High T_c Lead-Free Ba (Zr,Ti)O_3 Positive Temperature Coefficient of Resistivity Ceramic Using Impedance Spectroscopy. *International Journal of Mechanical Engineering and Applications.* Vol. 2, No. 1, 2014, pp. 11-17. doi: 10.11648/j.ijmea.20140201.13

Abstract: High T_c lead–free Ba ($Zr_{0.52}Ti_{0.48}$)O_3 positive temperature coefficient of resistivity (PTCR) ceramic was produced by the standard solid state reaction technique. X–ray diffraction pattern confirms the formation of the tetragonal perovskite structure of the ferroelectric sample. The conduction and relaxation mechanisms of the piezoelectric ceramic have been studied on the basis of activation energy. The relaxation mechanism is investigated for this sample based on the peaks of the imaginary part of electrical impedance and modulus spectra. The Cole-Cole plots indicate that the grain effect is influenced by the increase of temperature up to 200 °C and disappeared beyond this temperature. The temperature versus electrical resistivity plots show that a phase transition occurs at the Curie temperature, T_c =150 °C. The ceramic exhibits a PTCR jump of almost two orders of magnitude starting at 150 °C and ending at 275 °C with a high temperature coefficient of resistivity of ~25 % per °C. The electrical resistivity measurements also reveal that the sample shows semiconducting behavior beyond 275 °C with the value of negative temperature coefficient of resistivity of ~ 0.6% per °C.

Keywords: Relaxation Mechanism, Conduction Mechanism, Impedance Spectroscopy, Modulus Spectroscopy

1. Introduction

Perovskite–structured ferroelectric materials have the nominal formula ABO_3, where A is mono– or divalent ion with large radius and low valence, while B is a tetra– or pentavalent ion with very small radius and high valence. Among the perovskite-structured ferroelectric materials, $BaTiO_3$ is an insulating material with high electrical resistance (10^9–10^{13}) at room temperature with T_c = 130 °C. The insulating $BaTiO_3$ can be converted into semiconducting material by donor ions doping [1] and exhibits an abrupt increase in resistivity near T_c. This kind of behavior is commonly known as PTCR [2]. Lead-based perovskite piezoelectric materials have been studied extensively such as PMN–PT, PNN–PZT, PLZT, etc [3,4]. These kinds of piezoelectric materials have a lot of disadvantages because of their very high toxicity of lead. Due to this reason, researchers are recently interested in producing lead-free $BaTiO_3$–based materials for industrial applications. Barium titanate based Ba(Zr,Ti)O_3 (BZT) is one of the most important ceramic having perovskite ABO_3 structure with Zr in the A–site and Ti in the B–site. This material is an excellent candidate for variety of applications such as tunable filters, ring resonators, phase shifter, dynamic random access memories, tunable dielectric devices, multilayer ceramic capacitors, PTCR thermistors, etc [5,6] because it has local polar properties, the phase formation mechanism, dielectric and piezoelectric properties [7-9]. Several researchers have reported the PTCT effect in $BaTiO_3$ -based ferroelectric ceramics. The PTCR effect was first reported by Haayman et al. [10] in perovskite-structured $BaTiO_3$ materials containing a small amount of donors. The PTCR effect is described qualitatively by the Heywang model [11] and later amended by Jonker [12]. This description is based on the formation of surface acceptor states [13] at the grain boundary, which create a potential barrier due to the upward bending of the conduction band in the depletion region. Daniel et al. [14] investigated that the acceptors at the grain boundary layer

composed of Barium vacancies forming a 3-dimensional region spreading inside the grains. Saburi [15] studied semiconducting properties various donors doped $BaTiO_3$. Kangia [16] found that the PTCR effect in the ferroelectric materials is due to the surface charge layers formed at the grain boundaries. Although the PTCR effect in piezoelectric materials was revealed 50 years ago, the conclusive theory of this phenomenon is still not clear due to the convergence of both semiconducting and piezoelectric behaviors and intricate further by the polycrystalline nature of the material. From our best knowledge, the PTCR effect in BZT ceramics is less studied in the literature and not completely understood yet. Generally the conventional dc electrical measurements are used for characterizing the PTRC effect in BZT but these measurements give a little knowledge about this material. Both grain and grain boundary regions attribute to the electrical properties as well as PTCR effect of Barium $BaTiO_3$–based ceramics [17,18]. A better knowledge about the grain and grain boundary regions is needed to realize the origin PTCR effect in BZT ceramic. Therefore, the effect of grain and grain boundary region needs to be determined separately. Complex impedance investigation is regarded as an effective tool to separate the contributions of grains and grain boundaries regions to the general electrical properties of PTCR materials [19]. This article concentrates on the electrical conduction and relaxation mechanisms in high T_c lead free BZT PTCR ceramic using complex impedance and modulus spectroscopy in a wide frequency range (20Hz-1MHz) and at various temperatures (50-600°C).

2. Experimental Details

$BaZr_{0.52}Ti_{0.48}O_3$ samples were produced by the standard solid state reaction technique for different experimental measurements. The samples were produced by taking high purity $BaCO_3$, TiO_2 and ZrO_2 as starting materials in their stoichiometric proportions. The oxide materials were mixed properly by high energy ball milling. The powder mixtures were thoroughly ground in an agate mortar for couple of hours and then calcined at 950°C for 5 hours in an alumina crucible. The calcined powder was crushed again to obtain fine powder form. The product was mixed with proper amount (2/3 drops) of polyvinyl alcohol as a binder and then pressed at 145 MPa into disk shaped samples. The samples were then sintered at 1200°C for 5 hours in a programmable furnace. The thickness (0.16 cm) and area (1.121 cm^2) of the sintered samples were measured with the help of screw gauge. The samples were coated with silver paste on both sides to act as electrodes for electrical measurements. The complex impedance, modulus, and permittivity measurements were carried out using an impedance analyzer (WAYNE KERR 6500B) at oscillation amplitude of 0.5 volt.

3. Results and Discussion

3.1. Phase Identification

Fig. 1 illustrates the XRD pattern of BZT ferroelectric ceramic sintered at 1200 °C for 5 hours. The diffraction scan was performed by Cu-K_α radiation (λ=1.5415 Å) and noted within the range of $20 \le 2\theta \le 60$ degree. The peaks present in the XRD patterns are identified. The ceramic shows perovskite phase with tetragonal symmetry and there is no trace of additional secondary peaks. The tetragonal perovskite structure is investigated by (002)/(200) peak splitting by about 45 °C [20]. The lattice constants has been determined the predominant peaks at 2θ = 43.17, 45.26 correspond to (002) and (200) orientations. The values of lattice constants are found to be a=4.1129Å and c=4.1138Å.

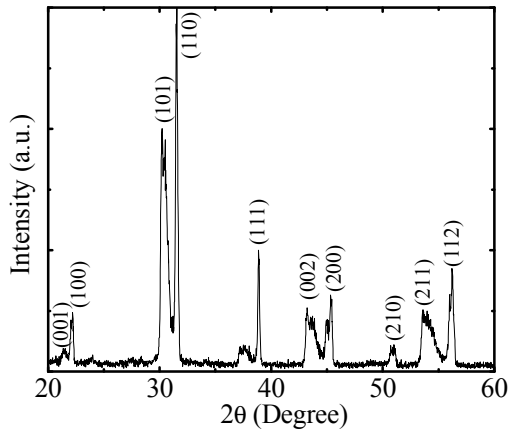

Fig 1. *X-ray diffraction pattern of BZT ceramic sintered at 1200°C.*

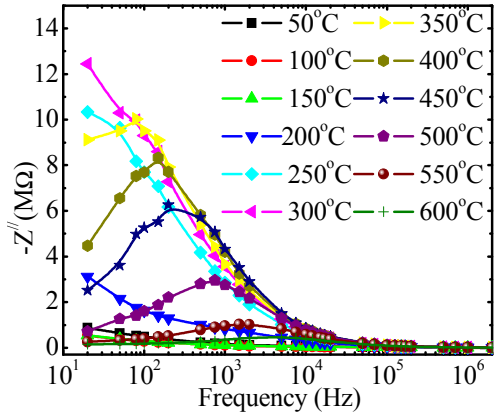

Fig 2. *Variation of imaginary part of the complex impedance with frequency for BZT ceramic at different temperatures.*

3.2. Relaxation Mechanism

We have used impedance, dielectric and modulus spectra to analyze relaxation mechanism in BZT ceramic. The real (Z') and imaginary (Z'') parts of the complex impedance $Z^* = Z' + iZ''$ have been calculated from measured capacitances (C) and resistances (R) data using the following equations [21]:

$$Z' = R/[1+(\omega RC)^2] \quad (1)$$

$$Z'' = \omega R^2 C/[1+(\omega RC)^2] \quad (2)$$

Fig. 2 shows the variation of Z'' as a function of frequency at different temperatures. Below 300°C, Z'' decreased gradually, demonstrating that relaxation phenomenon is absent in our measured frequency range. At and above 350 °C, the frequency response of Z'' graphs show a peak at a particular frequency known as relaxation frequency (f_{max}) and the peak position varies with temperature. The decrement in the magnitude of Z'' with increasing temperature indicates more conductivity due to the free charge in BZT material [22]**.** Therefore, the temperature dependent electrical relaxation mechanism subsists in this material. It is observed from the Fig. 2 that the merging of Z'' values at high frequency side is expected to the aggregation of space charge in this material. Fig. 3 shows the frequency response of dielectric permittivity (ε') at different temperatures. The ε' decreases steeply with increasing frequency without any relaxation peak, signifying relaxation is unavailable in dielectric spectra. It is regarded that the ε' decreases with increasing frequency exhibiting dispersion in the lower frequency region below 1 kHz. The ceramic shows dispersion due to Maxwell-Wagner [23] type interfacial polarization in approval with Koop's phenomenological theory [24]. A comparatively high value of ε' has been detected at very low frequencies. The high value of dielectric constant at lower frequencies is observed by heterogeneous conduction in this BZT ceramic [25]. At low frequency zone, dipoles follow the slow variation of the alternating electric field. As the frequency increases, dipoles start to lag behind the electric field and the ε' decreases. When frequency reaches at a certain frequency ($\omega = 1/\tau$), the dielectric constant drops. At higher frequency, the constant value of ε' is nearly observed, manifesting dipoles can no longer obey the first reversal of alternating electric field. The inset of Fig. 3 illustrates the variation of dielectric loss $(\tan\delta)$ as a function of frequency at several temperatures. The variation of $\tan\delta$ with frequency point out the similar dispersion in the low frequency region as ε' without any relaxation peaks. In the present ceramic, the large value dielectric loss occurs at the lower frequency by the virtue of space charge polarization. The periodic variation of the alternating electric field is very fast at higher frequency region so that there is no extra charge diffusion in the direction of the alternating electric field, demonstrating the abatement of the growth of charge carrier. So, the value of dielectric loss decreases as a result of the decrement of charge accumulation. Since the relaxation peak is not present in the dielectric spectra, we have studied the impedance spectroscopy for better understanding the relaxation mechanism in BZT ceramic. It has been demonstrated that the electric modulus represents the real dielectric relaxation process [23]. The electrical modulus has been calculated from impedance data using the following equation [21]:

$$M^* = M' + jM'' = j\omega C_o Z^* \quad (3)$$

Through the Equation (3), we can calculate the value imaginary (M'') part of the electric modulus using the relations: $M'' = \omega C_o Z'$. Fig. 4 illustrates frequency response curves of M'' spectra. It is stated form the Fig. 4 that the anomalous relaxation peaks are observed up to 425 ℃ and beyond this temperature, the peak is shifted toward the higher frequency side with increasing temperature, implying the relaxation is thermally activated process. The observed peaks turn to shift with increasing temperature expected to decrease relaxation time in this material. It is also noticed that the value of M'' in the high frequency region increases with increasing temperature. The f_{max} is depended on temperature and associated to the nature and strength of the electrical relaxation phenomenon in the material. The obtained relaxation frequencies in impedance spectra differ from the relaxation frequencies of the modulus spectra, specifying that the relaxation phenomenon in BZT material is non-Debye type. The values f_{max} for both the impedance and modulus spectra have been determined from the frequency versus M'' and Z'' plots. The temperature dependence of f_{max} is explained on the basis of Arrhenius relation. The values f_{max} follow the Arrhenius relation governed by the equation,

$$f = f_o \exp(-E_a / K_B T) \quad (4)$$

where f_o is the pre-exponential factor, K_B is Boltzmann constant and T is absolute temperature. Fig. 5 represents the Arrhenius plot of the relaxation frequencies for both the impedance and modulus. The values activation energy (E) have been determined from the slope of straight lines (Fig.5) and found to be 0.44 and 0.46 eV for impedance and modulus, respectively. We have monitored that the values E obtained from the relaxation frequencies of impedance and modulus spectra are almost same, therefore it may be assumed that the E is a convenient criterion for investigating the relaxation phenomenon in BZT material.

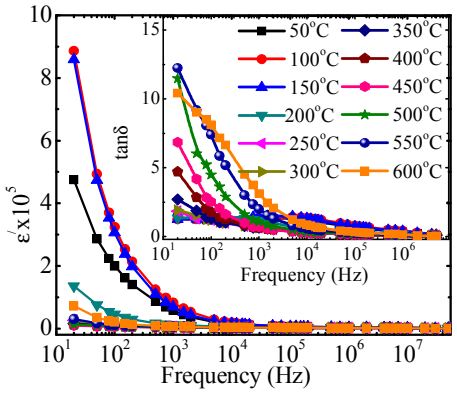

Fig 3. *Frequency response of the real part of permittivity and tangent loss (inset) of BZT ceramic at different temperatures.*

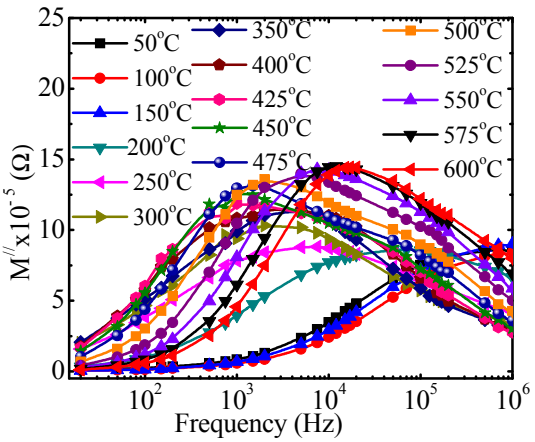

Fig 4. *Variation of imaginary part of modulus with frequency of BZT ceramic at different temperatures.*

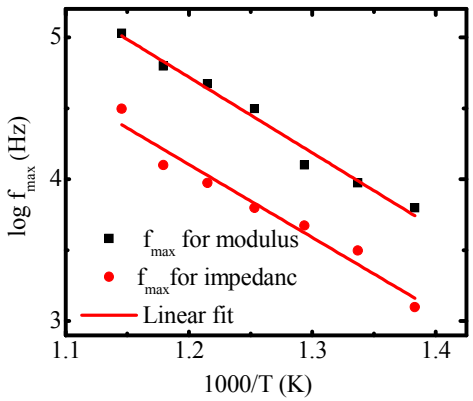

Fig 5. *Arrhenius plot of relaxation frequencies of imaginary impedance and modulus.*

3.3. Conduction Mechanism

To describe the origin of the PTCR effect in the BZT samples, complex impedance was utilized for investigating the resistivity of this ceramic. Fig. 6 illustrates the Cole-Cole plots of this ceramic at different temperatures. Two semicircular arcs have been detected from 50 to 200°C in Cole-Cole plots. The small semicircular arc in the higher frequency region is due to the grain effect and the large semicircular arc in the relatively low frequency region is the result of grain boundary effect. At 225 °C, the higher frequency semicircular arc disappears and a single semicircle is detected in the temperature range 225-600 °C, indicating the grain boundary effect dominates the PTCR ceramic in this temperature range. It is well known that the values of resistivity for grain (ρ_g) and grain boundary (ρ_{gb}) can be determined from the intercepts on the Z' axis of Z' versus Z'' plots at low and high frequencies respectively. Maiti et al. [26] have reported that an extra semicircular is observed in the Cole-Cole plots as a result of the electrode in the sample interface but the electrode used in present research work provide a good electrical contact and the interface resistivity can be negligible. The additional semicircle is the result of grain boundary region instead of the electrode in the sample interface. Therefore, both the grain and grain boundary have provided to the entire dc resistivity of this BZT sample. The temperature dependence of ac resistivity at various frequencies and the dc resistivity obtained from grain and grain boundary are illustrated in Fig. 7 (a) and (b), respectively. Both the values of ac and dc resistivity of BZT material below a critical temperature (150 °C) temperatures known Curie Temperature (T_c) is small compared to the other regions of temperature and slightly decreases up to T_c, indicating semiconducting behavior with a negative temperature coefficient of resistivity (NTCR). The low value of resistivity below T_c can be explained on the basis of Jonker model [12]. Below T_c, the resistivity is small due to the reduction of spontaneous polarization at the grain boundary barrier. In the present BZT ferroelectric ceramic, the piezoelectric domains of each crystal are spontaneously polarized. In the tetragonal perovskite structure, the BZT is a piezoelectric material with the direction of the polarization along the tetragonal axis. The polarization direction is distinctive from grain to grain. This is because each neighboring grain has a specific crystal orientation. The domain formation is not strained at the contact between two crystals of specific orientation and the polarization is not continuous through the surface of the sample. Since this is not desirable, domain structures are formed in such a way that the half of domain contains the negative surface charge of confined electrons compensates the difference in the perpendicular component of polarization on each sides of the boundary, and depletion layer is diminished. For the other half of the domains containing positive charge carriers, the potential barriers are strengthen by the ferroelectric domains, but since these are electrically in parallel, a overall small resistance is observed below T_c. A rapid increase in resistivity beginning at 150°C and ending at 275°C is observed in BZT ferroelectric ceramic. This abrupt increase in resistivity is accredited to the conversion from tetragonal ferroelectric phase to cubic paraelectric phase, which is manifestation of the PTCR effect. The PTCR magnitude, defined as $\rho_{\max}/\rho_{\min}$, where $\rho_{\max}$ is the maximum resistivity is observed above T_c and $\rho_{\min}$ is the minimum measured value resistivity occurring just below T_c. The PTCR jumping ratio of the BZT ferroelectric ceramic is $(\rho_{\max}/\rho_{\min}) \cong 10^{1.6}$. The unusual increase in resistivity can be explained on the basis of Heywang model [27]. Beyond T_c, the BZT is in the paraelectric state, the permittivity of the grain boundary follow the Curie-Weiss law is governed by the equation [27], $\varepsilon = C/T - T_c$, where C is curie constant and T is absolute temperature. The permittivity of the grain boundary decreases with increasing temperature and the equivalent potential barrier of this BZT material increase. For to this reason the resistivity enhances rapidly which depends exponentially on the potential barrier as governed by formula [27], $\rho = A\exp(\varphi/KT)$, where A is a geometrical factor, k is

Boltzmann constant. The energy of the localized electrons in the grain boundary rises with temperature together with the potential barrier until the Fermi level. The ρ_{max} is observed at 275 °C and beyond this temperature the resistivity again decrease because more increase of temperature causes a reduction of the surface charge due to a decrease in the density of trapped electrons, as a result φ become saturate and ρ begins to decrease. Therefore, the BZT ceramic exhibits metallic behavior from T_c to 275 °C with a high positive temperature coefficient of resistivity (α_p) of ~25 % per °C and semiconducting nature above 275 °C with a value of negative temperature coefficient of resistivity (α_n) of ~ 0.6% /°C. The activation energies has been determined from three different temperature regions such as below T_c (50-150 °C) , PTCR region (175-275 °C) and NTCR region (300-600 °C) using Arrhenius relation defined by the equation,

$$\rho = \rho_o \exp(-E/kT) \quad (5)$$

The values of E for both grain boundary resistivity and ac resistivity have been determined from the slope of the $\log\rho$ versus inverse of temperature plots (Fig.8). The obtained values are presented in the Table 1. It is observed from the Table 1 that the value of E obtained from grain boundary resistivity and ac resistivity are almost same for the three different temperature regions. Therefore, we may assume that the activation energy is a proper criterion for explaining the conduction mechanism in BZT ceramic.

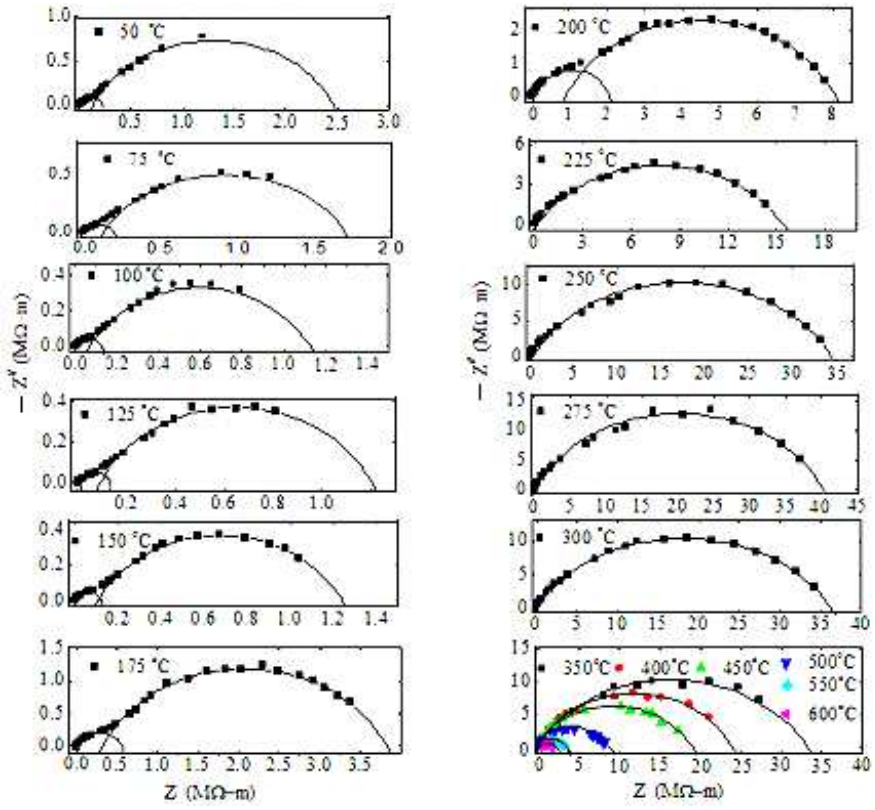

Fig 6. *Cole- Cole plots for BZT ceramic at different temperatures.*

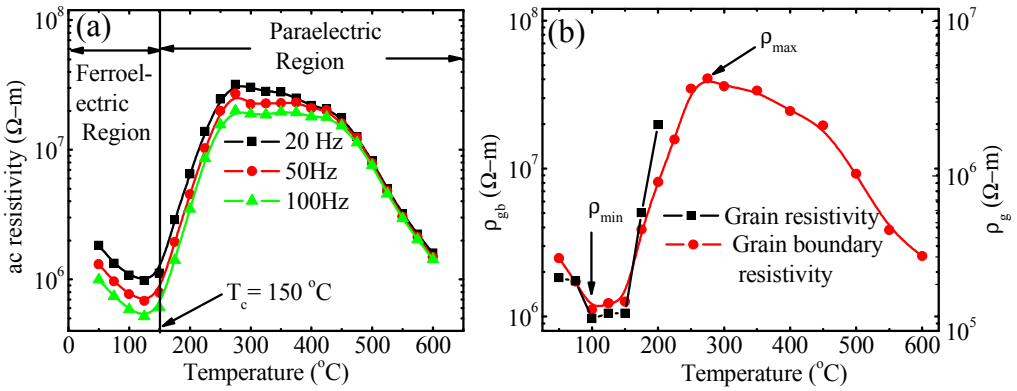

Fig 7. *Temperature dependence of (a) ac resistivity at different frequencies and (b) grain and grain boundary resistivity of BZT ceramic.*

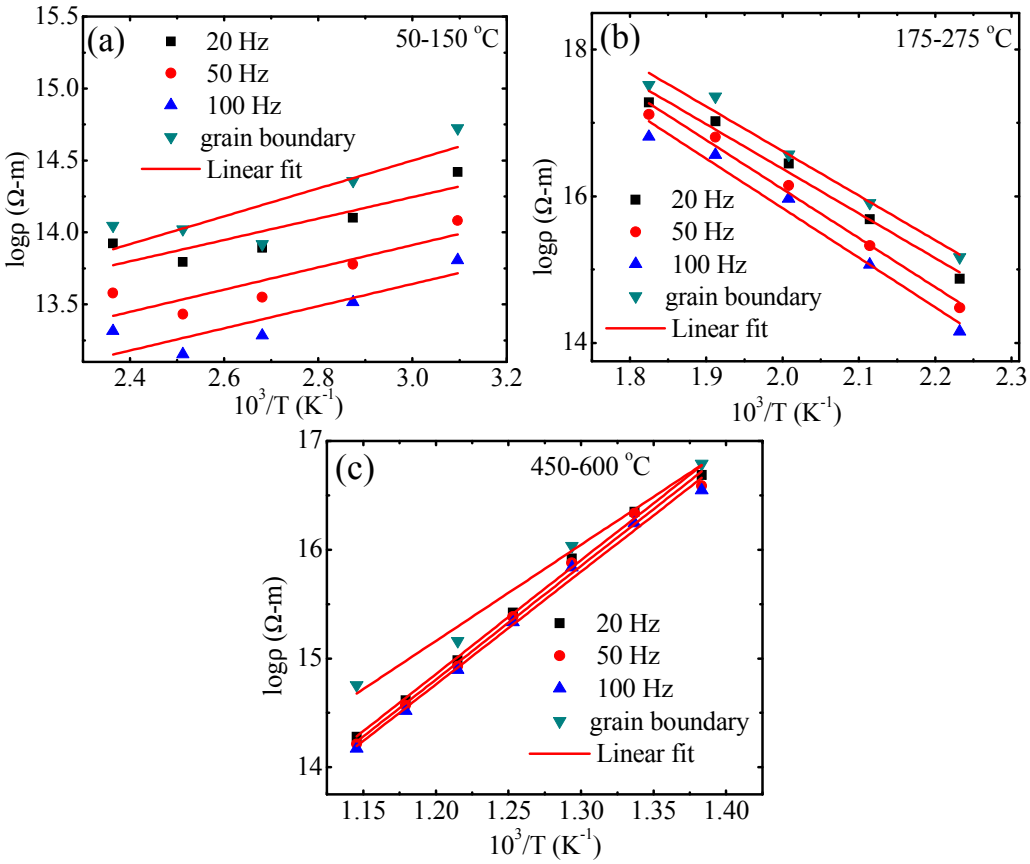

Fig 8. *Arrhenius plots of ac and grain boundary resistivity at different temperature regions (a) 50-150°C, (b) 175-275°C and (c) 450-600°C.*

Table 1. *Activation energy for grain boundary resistivity,* (E_{gb}) *ac resistivity and* (E_{ac}) *at different temperature ranges.*

Temperature ranges (°C)	E_{gb} (eV)	E_{ac} (eV) at 20 Hz	E_{ac} (eV) at 50 Hz	E_{ac} (eV) at 100 Hz
50-150	0.084	0.065	0.067	0.066
175-275	0.53	0.52	0.58	0.58
450-600	0.77	0.91	0.90	0.77

4. Conclusions

High T_c lead free $Ba(Zr_{0.52}Ti_{0.48})O_3$ ceramic was fabricated using the standard solid state reaction method. XRD pattern confirm the presence the tetragonal perovskite structure of this ceramic with lattice constants a = 4.1129Å and c = 4.1138Å. The obtained relaxations from the electric modulus and impedance are characterized by activation energy. The relaxation peaks shift to higher frequency side with increasing temperature, suggesting the relaxation phenomenon in BZT piezoelectric ceramic is thermally stimulated procedure. The dielectric permittivity shows dispersion below 1 kHz and almost constant beyond this frequency. Both grain and grain boundary resistivity have contributions to the PTCR effect of BZT ferroelectric ceramic. The maximum value of electrical resistivity is obtained at 275°C. The sample exhibits PTCR effect from 150 to 275ºC with a high value of temperature coefficient of resistivity. The PTCR jumping ratio of the BZT sample is $(\rho_{max}/\rho_{min}) \cong 10^{1.6}$. The remarkable PTCR effect is observed in this BZT ferroelectric ceramic, indicating that this ceramic may be a good candidate for lead-free PTCR thermistor applications.

Acknowledgement

The authors greatly acknowledge the Bangladesh University of Engineering and Technology (BUET) to provide financial support for this investigation.

References

[1] T. Lin, C. Hu, I. Lin, Journal of the American Ceramic Society 73 (1990) 531–536.

[2] P. Xiang, H. Takeda, T. Shiosaki, Applied Physics Letters 91 (2007) 162904.

[3] S.E. Park and T.R. Shrout, Journal of Applied Physics 82(1997)1804–1811.

[4] H. Fu, R.E. Cohen, Nature (London) 403 (2000) 281–283.

[5] U. Weber, G. Greuel, U. Boettger, S. Weber, D. Hennings, R. Waser, Journal of the American Ceramic Society 84 (2001) 759–766.

[6] F. Moura, A.Z. Simoes, B.D. Stojanovic, M.A. Zaghetea, E. Longo, J.A. Varela, Journal of Alloys and Compounds 462 (2008) 129–134.

[7] R. Farhi, M. Marssi, A. Simon, J. Ravez, European Physics Journal B 9 (1999) 599–604.

[8] K. Aliouane, A.G. Laidoudi, A. Simon, J. Ravez, Solid State Ionics 7(2005) 1324–1332.

[9] J. Bera, S.K. Rout, Materials Letters 59 (2005) 135–138.

[10] P. W. Haayman, R.R. Dam, H. A. Klassen, Geramn Patent Number 929 350 (1955).

[11] W. Heywang, Solid-State Electronics 3 (1961) 51–58.

[12] G. H. Jonker, Solid State Electronics 7 (1964) 895–903.

[13] W. Heywang, Journal of Materials Science 6 (1971)1214–1224.

[14] J. Daniels, K.H. Hardtl, R. Wenicke, Philips Technical Review 38 (1978/79) 73–82.

[15] O. Saburi, Journal of the Physical Society Japan 14 (1959) 1159–1174.

[16] K. Werner, Physics Review 82 (1955) 549-550.

[17] F.D. Morrison, D.C. Sinclair, A.R. West, Journal of the American Ceramic Society 84 (2001) 531–538.

[18] H. Beltrán, E. Cordoncillo, P. Escribano, D.C. Sinclair, A.R. West, Journal of Applied Physics 98, (2005) 094102.

[19] D.C. Sinclair, A.R. West, Journal of Materials Science 29 (1994) 6061-6068.

[20] M. Kosec, V. Bobnar, M. Hrovat, J. Bernard, B. Malic, J. Holc, Journal of Materials Research 19 (2004) 1849–1854.

[21] J. R. Macdonald, Impedance Spectroscopy, Wiley, New York, 1987.

[22] T.A. Nealon, Ferroelectrics 76 (1987) 377–382.

[23] J. C. Maxwell, Electricity and Magnetism, Oxford University Press, London, 1973.

[24] C.G. Koops, Physical Review 83 (1951) 121–124.

[25] C.A. Guarany, L.H.Z. Pelaio, E.B. Araujo, K. Yukimitu, J.C.S. Moraes, J.A. Eiras, Journal of Physics : Condensed Matter 15 (2003) 4851–4858.

[26] H. S. Maiti, R. N. Basu, Materials Research Bulletin 21(1986)1107–1114.

[27] W. Heywang, Journal of the American Ceramic Society, 47 (1964) 484–490.